



## Typhoon activity and some important parameters in the South China Sea



Tahereh Haghroosta<sup>a,b,\*</sup>, Wan Ruslan Ismail<sup>c</sup>

<sup>a</sup> Iranian Coastal & Marine Structural Engineering Association, Tehran, Iran

<sup>b</sup> Arman Darya Research-based Corporations, Tehran, Iran

<sup>c</sup> Section of Geography, School of Humanities, Universiti Sains Malaysia, 11800, Minden, Pulau Pinang, Malaysia

### ARTICLE INFO

#### Keywords:

Typhoon  
Sea surface temperature  
Latent heat flux  
Sensible heat flux  
Precipitation rate  
South China Sea

### ABSTRACT

This study aims to statistically describe temporal and spatial variations of sea surface temperature (SST), latent heat flux (LHF), sensible heat flux (SHF), and precipitation rate with typhoon activity over the South China Sea. The correlations of the parameters and their connections with the physical phenomena are clearly presented. This is fundamental to predict a typhoon's intensity and track. The effects were investigated from 1991 to 2011 based on archived data from the National Centers for Environmental Prediction and the National Center for Atmospheric Research (NCEP-NCAR) and the number of typhoons were sourced from the International Best Track Archive for Climate Stewardship (IBTrACS). The results showed that most typhoons occurred in August and September, which was related to high temperature in the summer season and the southwest monsoon in the area. The maximum mean values of SST in May and June were related to the East Asian Monsoon. The average values of LHF were highest in July, and the mean values of SHF were highest in July and August. SHF varied gradually at different months compared with LHF. In addition, the average of precipitation rate was highest in November, which can be related to the northeasterly winter monsoon. The relationships of the aforementioned parameters were obtained using Pearson's correlation analysis. Moreover, the highest and lowest mean values of the parameters in different areas were considered, and their spatial relationships were analyzed.

### 1. Introduction

Tropical cyclones (TCs) are large-scale destructive natural hazards that cause serious ecological and human damage. Heavy winds and rainfall from TCs could lead to severe disasters, such as storm surges and flooding. In fact, warm humid air is used as a reinforcement factor for huge “engine-like” TCs. Thus, TCs form over warm water in tropical areas (Anthes, 1986).

According to previous research, the energy source of storms is due to thermodynamical instability between the atmosphere and oceans in tropical areas (Emanuel, 1991). This is related to an actual temperature difference between air and water and also the air saturation of the near-surface. In addition, water evaporation transfers heat from the ocean with a large effective heat capacity in comparison to the atmosphere. Furthermore, among all parameters affecting TC generation and intensification, and from a thermodynamical point of view, SST and heat fluxes have essential roles to play in TC intensity and the cyclones development and stability (Emanuel, 2007; Yu and Weller, 2007).

Moreover, typhoons are important events in the South China Sea, which affect precipitation and cause enormous destruction. In particular,

precipitation from typhoons significantly contributes to overall precipitation and can cause disasters such as flooding, man-made disasters, and landslides (Shaluf, 2006). In addition, the movement of TCs over warm oceans represents an air-sea interaction. Some studies have been conducted on the effect of sea surface temperature (SST) on typhoon intensity in different years (Zuki and Lupo, 2008; Dare and McBride, 2011a, 2011b). Furthermore, the relationship between heat fluxes and SST and its importance were investigated in different studies (Park et al., 2005; McCulloch and Culverwell, 2005; Li et al., 2008). Yu and Weller (2007) analyzed a time series of daily latent and sensible heat fluxes during 1981–2005, over the global tropic oceans achieved from satellite and atmospheric reanalysis. They found that latent heat flux (LHF), and sensible heat flux (SHF), are essential parameters in the air-sea interaction. This matter was also represented by Clark (2004). However, limited literature on the interactions between typhoon intensity and parameters such as SHF and LHF is available; thus this study tries to specify those interactions in our chosen study area.

The results of a study by Haghroosta and Ismail (2016) showed that the initial SST value of different typhoons and the SST extent affected typhoon intensity and duration. Moreover, higher LHF caused more rain.

\* Corresponding author. Arman Darya Research-based Corporations, Tehran, Iran.  
E-mail address: [haghroosta@hotmail.com](mailto:haghroosta@hotmail.com) (T. Haghroosta).

When SHF anomaly was positive (negative), the initial SST value was highest (lowest). Thus, SST and SHF anomalies were positively correlated. Variations of SST, LHF, SHF, SLP, and precipitation rate and their anomalies in different typhoons were analyzed in the day on which a typhoon had its highest wind speed in comparison with the parameters during the first day. The results showed that temperature for the high-intensity day of typhoon reduced relative to the first day, indicating a typhoon-induced SST cooling effect.

The rest of the paper is organized as follows: the study area and the data used in temporal and spatial analysis are presented in Section 2. The methods are given in Section 3. Section 4 discusses the results. The last section presents the conclusion.

## 2. Data

### 2.1. Study area

South China Sea is the largest marginal sea located in the north-western Pacific Ocean, extending from the equator to 23 °N latitude and from 99 °E to 125 °E longitude (Fig. 1). The area is a semi-closed ocean basin surrounded by South China, Vietnam, Cambodia, Thailand, Peninsular Malaysia, Borneo Island, Indonesia, the Philippines, Taiwan, and the Indo-China Peninsula (Ho et al., 2000; Wang, 2008). The area connects with the east of China Sea, the Indian Ocean, and the Pacific Ocean through the Taiwan Straits, the Straits of Malacca, and the Luzon Straits, respectively. The South China Sea is one of the most important places for TC generation. In this paper, the study area is limited to 1 °N to 16 °N and from 100 °E to 130 °E, in latitude and longitude.

### 2.2. Data to determine temporal and spatial variations of selected parameters and typhoon activity

For long-term study, values of SST, precipitation rate, LHF, and SHF were obtained from the monthly mean and daily NCEP reanalysis data (Kalnay et al., 1996), available from the Climate Prediction Center (CDC), for the period 1991 to 2011. The dataset is valuable in forecasting and investigating extreme weather events (Grumm, 2005; Hamill et al., 2005). The global dataset has a horizontal grid spacing (resolution) of  $2.5^\circ \times 2.5^\circ$ . Data relating to typhoon numbers and exact locations were

obtained from the International Best Track Archive for Climate Stewardship (IBTrACS) dataset (Knapp et al., 2010). The typhoons were selected in consideration of their generation, development, and dissipation in the study area.

## 3. Methods

Statistical analyses were performed using SPSS 21.0 for Windows and significant levels for all analyses were set to 0.05. Normal distribution of data was determined based on Kurtosis and Skewness coefficients. After normal distribution was determined, multiple regression analysis was conducted to study the relationship between the number of typhoons and precipitation rate, SST, SHF and LHF. One-way analysis of variance (ANOVA) method was employed to determine the significant differences between the means of two or more independent parameters (Wilks, 2011). A significant difference between two parameters is determined if the p-value in the ANOVA table is less than 0.05.

In addition, parametric correlations were tested with Pearson's correlation test to establish the relationship between the aforementioned parameters and typhoon activity. Pearson's correlation coefficient (CC) higher than 0.5, indicates strong correlation (Explorable, 2008).

Moreover, the temporal relationships were analyzed between the monthly mean values of SST, LHF, SHF, precipitation rate (from NCEP-NCAR), and the number of typhoons (from IBTrACS). To investigate the spatial variations of the parameters with typhoon activity in different regions, the study area was divided into 10 equal sections geographically (A1 to A10). The map was drawn using Grads software (Fig. 2).

## 4. Results and discussions

### 4.1. Temporal variations

The mean values of the number of typhoons, SST, LHF, SHF, and precipitation rate were analyzed by the one-way ANOVA, and results showed significant differences for each parameter across different months ( $p < 0.05$ ). As shown in Fig. 3, the monthly mean values of number of typhoons from 1991 to 2011 are also significantly different ( $P < 0.05$ ). The number of typhoons had a maximum monthly mean value of  $2 \pm 0.6$ . The error bar in the figure stands for standard deviation.

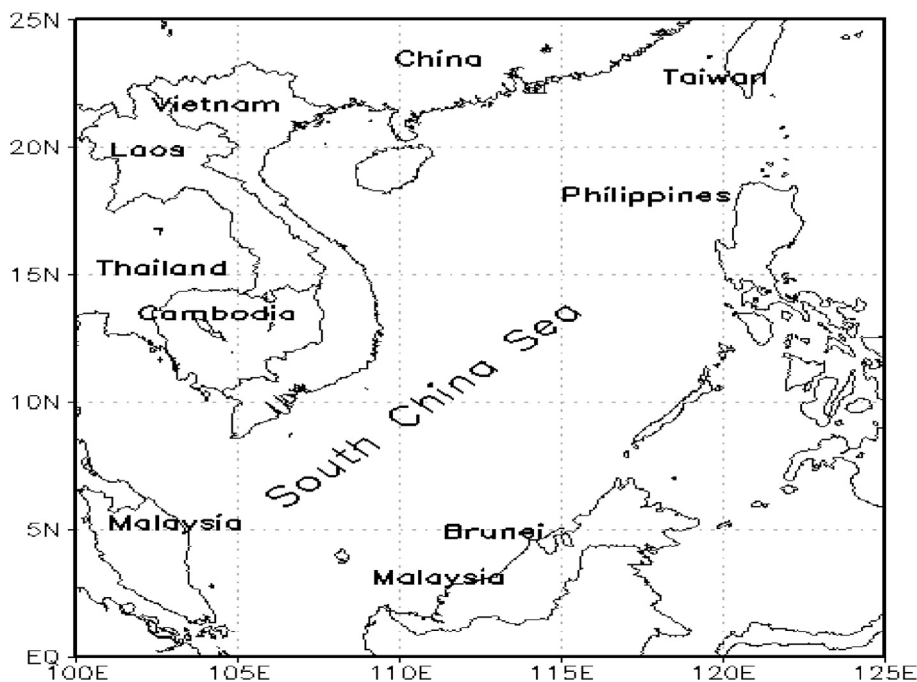


Fig. 1. South China Sea.

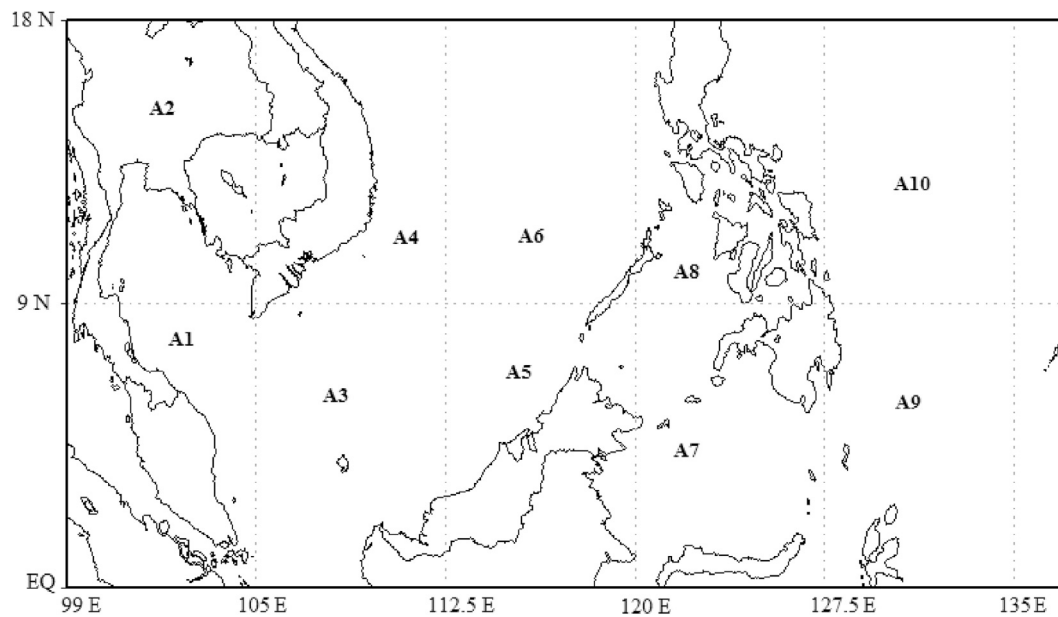


Fig. 2. Defined regions in study area.

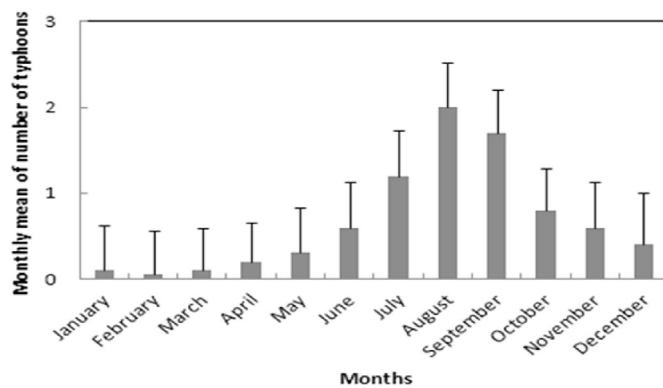


Fig. 3. Monthly mean values of number of typhoons in the South China Sea (1991–2011). The error bar stands for standard deviation.

Fig. 3 illustrates that the maximum number of typhoons occurred in August and September, which could be related to high temperatures in the summer season and the southwest monsoon in the area. The maximum in August and September agrees with the results of Wang (2008) who analyzed the period 1945 to 2005. The number of typhoons showed a decreasing trend from August to December, which can be relevant to low temperature in rainy season. Furthermore, Vongvisessomjai (2009) reported that the number of TCs decline in October, November, and December, which concur with the results of the present study. However, this outcome is different from the observations of Zuki and Lupo (2008), which showed November and December as the most active months from 1960 to 2006. The shift may be due to the differentiation between the periods of the two studies (i.e., the present work covers 1991–2011).

The temporal variations of SST across different months (Fig. 4) showed an increasing trend from January to May and a decreasing trend from June to December. In agreement with Shaw et al. (2011), the onset of the summer monsoon was marked by a period of pre-monsoonal rain over South China and Taiwan in early May. The highest SST values were in May and June with amounts of  $27.73 \pm 0.24$  and  $27.68 \pm 0.26$ , respectively. The highest temperature can be due to the existence of East Asian Monsoon in the area which is driven by temperature differences between the Asian continent and the Pacific Ocean. Moreover, the

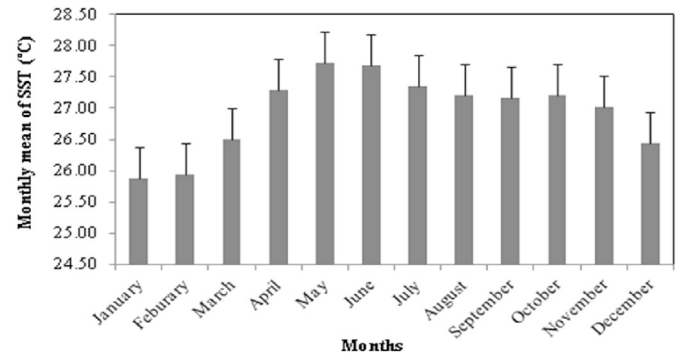


Fig. 4. Monthly mean values of SST (°C) in the South China Sea (1991–2011). The error bar stands for standard deviation.

one-way ANOVA analysis confirmed the results ( $p < 0.05$ ), which represent significant differences across different months.

The monsoon trough is located north of the equator in December (Krishnamurti, 1979) and it is a shear-line separating the westerly monsoon from trade easterlies. The results are in agreement with the findings of Wang (2008) who reported a decreasing SST trend in the South China Sea from September to December for the period of 1945–2005.

Furthermore, the increasing trend from January to May is in agreement with the warming trend reported by Wang et al. (2013) and Kuo and Lee (2013) for the months of February and May in the South China Sea. This particular warming could be a result of heat advection by the westward movement of fronts as an effect of the northeasterly winter monsoon. Belkin and Lee (2014) reported a warming trend from January to March and a cooling trend from July to September. Furthermore, the East Asian winter monsoon appears as one of the most important factors that controlling the regional climate in the area.

The variations of monthly mean values of LHF and SHF are illustrated in Figs. 5 and 6. The amount of LHF fluctuates between different months, with the highest value in July ( $111.66 \pm 11 \text{ W/m}^2$ ) and minimum value in October ( $98.47 \pm 8.2 \text{ W/m}^2$ ). Significant differences across months were confirmed by the one-way ANOVA ( $p < 0.05$ ). SHF had the highest values in July and August ( $9.4 \pm 2.8$ , and  $8.9 \pm 1.8 \text{ W/m}^2$ , respectively). In addition, the one-way ANOVA showed a significance difference across

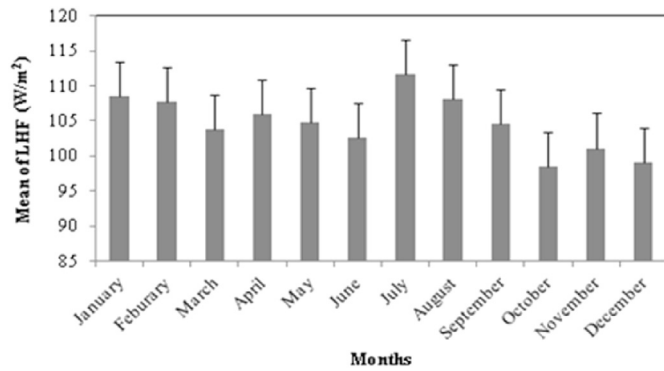


Fig. 5. Monthly mean variations of LHF (W/m<sup>2</sup>) in the South China Sea (1991–2011). The error bar stands for standard deviation.

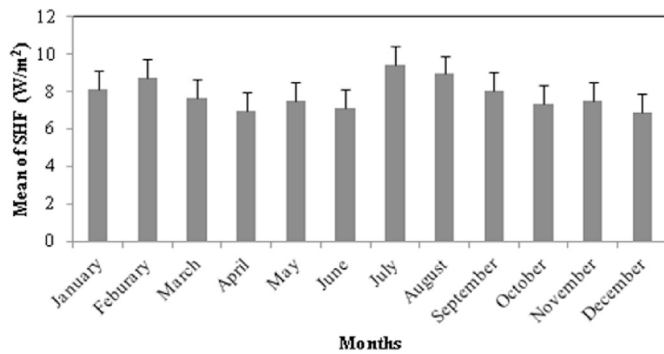


Fig. 6. Monthly mean variations of SHF (W/m<sup>2</sup>) in the South China Sea (1991–2011). The error bar stands for standard deviation.

months ( $p < 0.05$ ). SHF varied more with a gradual slope for different months compared with the LHF. The gradual slope of SHF in the area was also observed by Zong et al. (2010) who studied the LHF and SHF in the South China Sea.

The variations of precipitation rate across different months from 1991 to 2011 (Fig. 7) showed an increasing trend from February to November. The highest monthly mean precipitation rate was in November with an amount of  $1.07E-05 \pm 1.31E-05 \text{ kg/m}^2/\text{s}$ .

The highest value of rainfall may be connected to the northeasterly winter monsoon. The lowest amount of rainfall was also mentioned by Yuan and Miller (2002), but the highest value was different from theirs, which indicated that the maximum rainfall occurring in August in northern hemisphere. The difference may be related to that they investigated the rainfall globally and used another dataset for the rainfall.

Pearson's correlation for all parameters indicated that there were

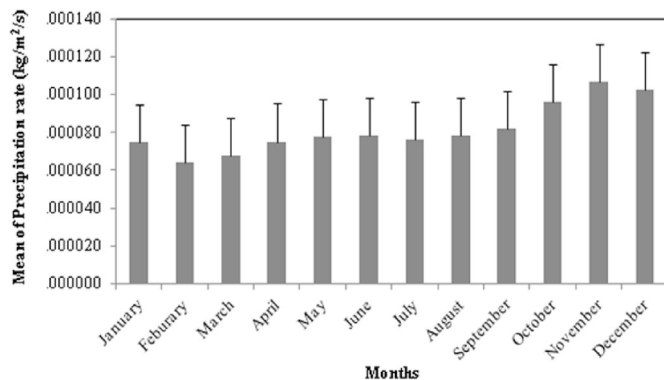


Fig. 7. Monthly mean variations of precipitation rate (kg/m<sup>2</sup>/s) in the South China Sea (1991–2011). The error bar stands for standard deviation.

negative correlations for the three-month mean values (July, August, and September) of the number of typhoons versus SST ( $CC = -0.44$ ) at 0.05 level of significance. The negative correlation is related to the cooling effect in the typhoon season. The effect is due to temperature reduction after typhoon's passage in the area.

The monthly mean values of LHF and the number of typhoons also showed a negative correlation ( $CC = -0.32$ ) during the months of July, August, and September. This finding represents the elimination of LHF from the atmosphere and its absorption by the ocean, thereby weakening the TCs. In fact, the air-sea interface heat exchange of TCs was very strong; LHF was also the main contributor to heat.

The monthly mean values of SHF and the number of typhoons showed a strong positive correlation ( $CC = 0.51$ ) for the months of October, November, and December. The findings indicate that SHF when cyclones occurred significantly increased during these months. A weak correlation of SHF and number of typhoons was also observed in summer. The correlation can be due to the fact that increasing the amount of heat can generate more typhoons. The results of the present study complement the findings of Liu et al. (2012).

Bender et al. (1993) observed a decrease of total heat flux in relation to typhoon activity over the area. In other words, the cooling effect by the typhoon resulted in a significant effect on the storm intensity due to the reduction of total heat flux directed into the typhoon above the regions of SST reduction.

A weak negative correlation was found between the monthly mean values of number of typhoons and precipitation rate from January to September ( $CC = -0.34, -0.23, \text{ and } -0.18$ , respectively for three-monthly averages) and a positive correlation from October to December ( $CC = 0.35$ ) at the 5% significance level. The correlations between the number of typhoons and precipitation rate represent the rainy and dry seasons in the area. The current findings were also similar to those obtained by Zhai et al. (2005). Based on the results, SST is enhanced before a typhoon, while precipitation rate is increased after a typhoon. The results indicate that SST in the area increases before a typhoon occurrence to prepare its required energy, thereby causing the typhoon to bring additional precipitation in subsequent months. The same result was confirmed by Uram (2005), who explained the process of heat condensation and the use of heat fluxes as fuel for typhoons. Zhang et al. (2014) also reported that the sea-surface is a major energy source for TC development and maintenance. In fact, higher SSTs can fuel stronger TCs.

#### 4.2. Spatial variations

A spatial investigation of the mean values of SST, LHF, SHF, and precipitation rate during the period of 1991–2011 was conducted in different regions. The one-way ANOVA showed significant differences in all areas for the parameters ( $p < 0.05$ ).

The mean values of SST in different areas (Fig. 8) are significantly different. The highest value of SST was in area 9 (A9) with amounts of  $29.17 \pm 0.19 \text{ }^\circ\text{C}$ . The range of mean values of SST was from  $25.29 \text{ }^\circ\text{C}$  (A2) to  $29.17 \text{ }^\circ\text{C}$  (A9).

Fig. 9 shows that the mean values of LHF in different areas are significantly different. The highest value of LHF was in A10 with an amount of  $141.88 \pm 8.76 \text{ W/m}^2$ . The range of mean values of LHF was from  $93.03 \text{ W/m}^2$  (A7) to  $141.88 \text{ W/m}^2$  (A10).

The mean values of SHF in different areas are shown in Fig. 10. Significant differences were observed between areas ( $p < 0.05$ ), which may be related to the considerable fluctuations for the different areas. The same finding was reported by Ginis (2002), who observed the presence of SST fluctuations with heat fluxes. The highest value of SHF was in A2 with  $18.67 \pm 7.79 \text{ W/m}^2$  (i.e., more land mass). The SHF mean values ranged from  $6.42 \text{ W/m}^2$  (A7) to  $18.67 \text{ W/m}^2$  (A2).

The mean values of precipitation rate in different areas are shown in Fig. 11. The highest values were in the A9 region with  $8.69E-05 \pm 1.08E-05 \text{ kg/m}^2/\text{s}$  while the lowest value was in A7 with  $5.96E-05 \text{ kg/m}^2/\text{s}$ .

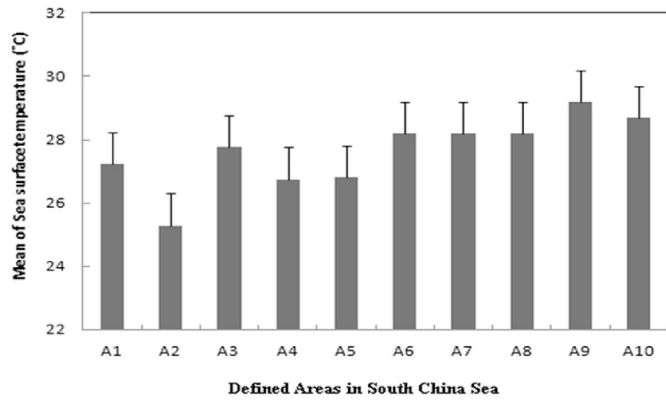


Fig. 8. Mean values of SST (°C) in different areas in the South China Sea (1991–2011). The error bar stands for standard deviation.

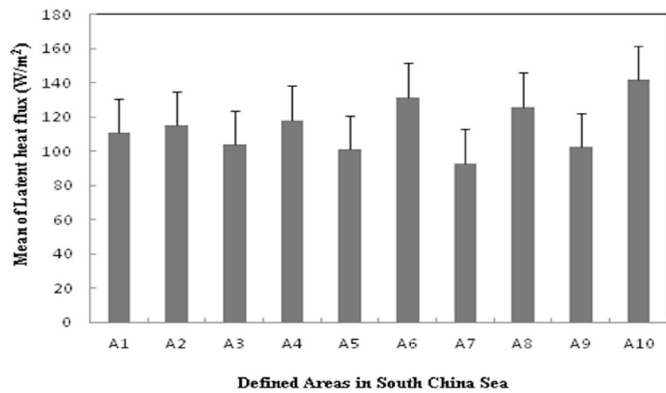


Fig. 9. Mean values of LHF (W/m<sup>2</sup>) in different areas in the South China Sea (1991–2011). The error bar stands for standard deviation.

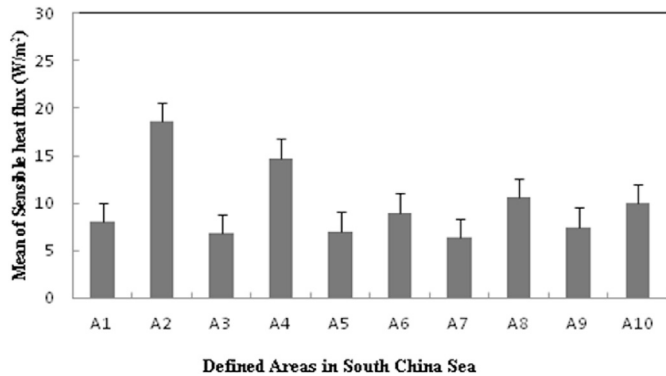


Fig. 10. Mean values of SHF (W/m<sup>2</sup>) in different areas in the South China Sea (1991–2011). The error bar stands for standard deviation.

Lower latitudes receive more precipitation because they are located in wet regions within inter-tropical convergence zones and the equatorial Pacific Ocean. The results agree with the finding of Yuan and Miller (2002) in studying the seasonal variation of precipitation patterns in the global ocean.

The average number of typhoons occurring in the region is illustrated in Fig. 12. The areas of A6, A8, and A10, which are located in high latitudes and longitudes, had the highest number of typhoons. The areas in the lowest latitudes and longitudes (A1 to A5) had lowest number of typhoons because these areas have more landmass and the Coriolis force is weakest in them.

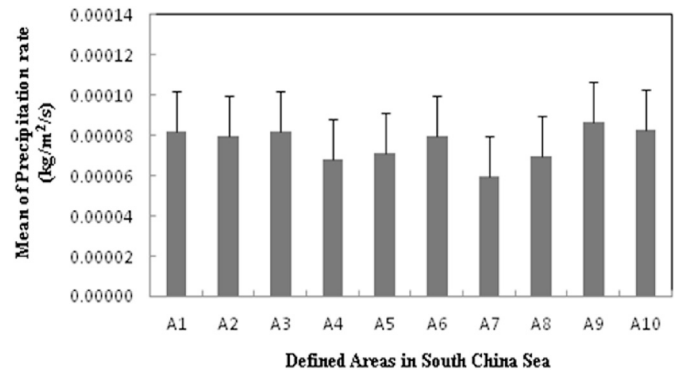


Fig. 11. Mean values of precipitation rate (kg/m<sup>2</sup>/s) in different areas in the South China Sea (1991–2011). The error bar stands for standard deviation.

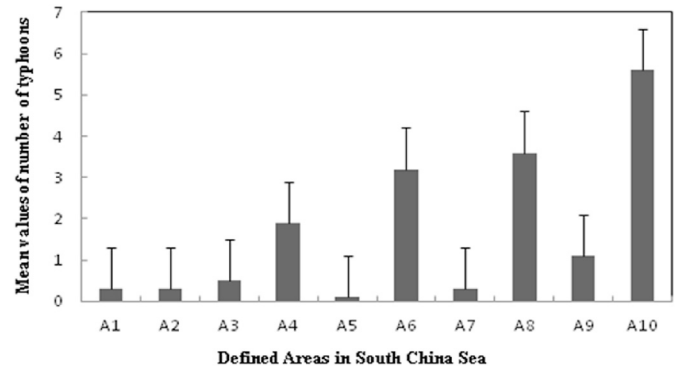


Fig. 12. Average number of typhoons in different areas in the South China Sea (1991–2011). The error bar stands for standard deviation.

Pearson's correlation on all parameters in the areas showed that SST had a strong negative correlation with LHF and precipitation rate (CC = −0.75, and −0.92, respectively) in A1, but switched to a positive correlation in A4 (CC = 0.48 and 0.50, correspondingly), which may be related to the development of summer monsoon in the region. The same relationship was also observed by Zeng et al. (2009), who reported that as the summer monsoon develops, a strong wind jet occurs. Similarly, high LHF and large specific humidity differences was observed in this area. Furthermore, in agreement with the findings of Deng et al. (2014), the summer monsoon strongly influences precipitation over the South China Sea. The negative correlation between SST and precipitation rate was also confirmed by Emanuel and Sobel (2013) when they investigated the variations of tropical SST, and precipitation by the global and local forcing. The correlation may be related to the increased transmission of longwave radiation from the surface directly to space through a dry troposphere. The relationship established by the present study is also in agreement with Cha and Lee (2009), who explained the relation of a subtropical high, and high precipitation over the South China Sea in the dry season, and its subsequent westward movement to the North Pacific (Deng et al., 2014). Thus, the impact of SST on the atmosphere over the area is weaker than the effect of the atmosphere on SST.

Findings further showed that SST had a strong negative correlation with SHF in A4 (CC = −0.58) because of the reduction of SHF from the ocean to the atmosphere in warmer areas, as confirmed by the previous works of Nan et al. (2009) and Liu et al. (2012) in studying the Indian Ocean sea surface temperature, and East Asian summer monsoon. The correlation between LHF and precipitation rate was strongly positive (CC = 0.75 on average) in these areas at the 5% significance level, which may be due to summer monsoon expansion in the area as confirmed by Zeng et al. (2009) in evaluating a satellite-derived latent heat flux product in the South China Sea.

In areas with higher latitudes and longitudes (A6, A8, and A10) where

the number of typhoons was greatest, the SST and SHF had a strong negative correlation ( $CC = -0.87$ ,  $-0.54$ , and  $-0.81$ ), which indicates that the ocean eliminates heat fluxes from the atmosphere and causes weakening in typhoons. The same finding was also mentioned by Liu et al. (2012). The negative SHF occurred within the typhoon circulation in warm conditions, and the SHF of the typhoon significantly increased in less warm areas. Additionally, SST and precipitation rate had a strong positive correlation ( $CC = 0.48$ ,  $0.59$ , and  $0.77$ ), which aligns with the findings of Xie et al. (2010). Increased precipitation occurs when SST increases (“warmer becomes wetter” rule). In the A10 region, the area with the highest number of typhoons, the correlations of LHF with SHF and precipitation rate were positively significant ( $CC = 0.85$ , and  $0.97$ ) because of strong air-sea heat exchanges and due to the LHF, which was the main contributor of heat. The air-sea interface heat exchange of TCs is also very strong because of LHF providing heat and moisture. The same findings were reported stated by Liu et al. (2012). Cayan (1992) and Gao and Xie (2014) also showed a positive correlation in their studies.

## 5. Conclusion

The current study focused on the statistical analyses, investigated the effective parameters in typhoon generation from temporal and spatial point of views, and explored some correlations between them as follows. The findings can help researchers to predict typhoons in advance.

Analysis was conducted to show the relation of typhoon activity with the parameters of SST, LHF, SHF, SLP, and precipitation rate for the period of 1991–2011. Results showed that most typhoons occurred in August and September. The study presented some conditions to explain why the selected parameters provide a proper environment for typhoon activity. The maximum mean values of SST occurred in May and June. The SST also showed an increasing trend from January to May and decreasing trend from June to December, which are influenced by the summer monsoon (monsoon trough in December) and pre-monsoonal rain over South China. The average values of LHF were highest in July and lowest was in October. The mean values of SHF were highest in July and August. The SHF varied more with gradual slope during different months compared with LHF. The average value of the precipitation rate was highest in November and lowest in February, which is affected by the northeasterly winter monsoon.

Correlations were established for the aforementioned parameters and typhoon activity. A negative correlation indicates that the factors change in reverse, while a positive correlation implies that the parameters vary in accordance with each other. A negative correlation was established for the monthly values of number of typhoons and SST in July, August, and September. In addition, a negative correlation was found for the monthly mean values of the number of typhoons and precipitation rate from January to September, while a positive correlation was found from October to December. The monthly mean values of LHF and number of typhoons showed a negative correlation in July, August, and September. While the monthly mean values of SHF and number of typhoons showed a positive correlation in October, November, and December. A weak correlation for the SHF occurred during the typhoon season in summer.

A spatial investigation of the mean values of SST, LHF, SHF, and precipitation rate showed significant differences in various areas. Lower latitudes received more precipitation than other areas. Areas in high latitudes and longitudes had the highest number of typhoons, while areas in lowest latitudes had the lowest average number of typhoons. SST had a strong negative correlation with LHF and precipitation rate in areas with lower longitudes and latitudes, and the relation of SST, LHF, and precipitation rate shifted from a negative to a positive correlation.

## Acknowledgements

The Authors would like to thank to Dr. Fereshteh Saraji and Dr. Seyedeh Laili Mohebbi Nozar, for their guidance in statistical analysis.

## References

- Anthes, R.A., 1986. Tropical Cyclones Their Evolution, Structure and Effects. American Meteorological Society, Boston, MA.
- Belkin, I.M., Lee, M.A., 2014. Long-term variability of sea surface temperature in Taiwan Strait. *Clim. Change* 124, 821–834.
- Bender, M.A., Ginis, I., Kurihara, Y., 1993. Numerical simulations of tropical cyclone-ocean interaction with a high-resolution coupled model. *J. Geophys. Res.* 98, 23–27.
- Cayan, D.R., 1992. Latent and sensible heat flux anomalies over the northern oceans: driving the sea surface temperature. *J. Phys. Oceanogr.* 22, 859–881.
- Cha, D.H., Lee, D.K., 2009. Reduction of systematic errors in regional climate simulations of the summer monsoon over East Asia and the Western North Pacific by applying the spectral nudging technique. *J. Geophys. Res.* 114, 1–17. D14108/.
- Clark, J.O.E., 2004. *The Essential Dictionary of Science*. Barnes & Noble Books, New York.
- Dare, R.A., McBride, J.L., 2011a. Sea surface temperature response to tropical cyclones. *Mon. Weather Rev.* 139, 3798–3808.
- Dare, R.A., McBride, J.L., 2011b. The threshold sea surface temperature condition for tropical cyclogenesis. *J. Clim.* 24, 4570–4576.
- Deng, Y., Gao, T., Gao, H., Yao, X., Xie, L., 2014. Regional precipitation variability in East Asia related to climate and environmental factors during 1979–2012. *Sci. Rep.* 4, 1–13.
- Emanuel, K.A., 2007. Environmental factors affecting tropical cyclone power dissipation. *J. Clim.* 20, 5497–5509.
- Emanuel, K.A., 1991. The theory of hurricanes. *Annu. Rev. Fluid Mech.* 23, 179–196.
- Emanuel, K., Sobel, A., 2013. Response of tropical sea surface temperature, precipitation, and tropical cyclone-related variables to changes in global and local forcing. *J. Adv. Model. Earth Syst.* 5, 447–458.
- Explorable, 2008. Statistical Correlations [Online]. Available: [Accessed 30 September 2014]. <http://www.explorables.com/statistical-correlation>.
- Gao, T., Xie, L., 2014. Multivariate regression analysis and statistical modeling for summer extreme precipitation over the Yangtze river basin, China. *Adv. Meteorol.* 2014, 269059/1–8.
- Ginis, I., 2002. Tropical cyclone-ocean interactions. *Adv. Fluid Mech.* 33, 83–114.
- Grumm, R.H., 2005. Examining Severe Weather Events Using Reanalysis Datasets. 21<sup>st</sup> Conference on Weather Analysis and Forecasting/17<sup>th</sup> Conference on Numerical Weather Prediction. American Meteorological Society, Washington, DC.
- Haghroosta, T., Ismail, W.R., 2016. Investigating short-term variations of some parameters during the selected typhoons in the South China Sea. *Res. Mar. Sci.* 1, 13–21.
- Hamill, T.M., Schneider, R.S., Brooks, H.E., Forbes, G.S., Bluestein, H.B., Steinberg, M., Meléndez, D., Dole, R.M., 2005. The May 2003 extended tornado outbreak. *Bull. Am. Meteorol. Soc.* 86, 531–542.
- Ho, C.R., Zheng, Q., Soong, Y.S., Kuo, N.J., Hu, J.H., 2000. Seasonal variability of sea surface height in the South China Sea observed with TOPEX/Poseidon altimeter data. *J. Geophys. Res.* 105 (C6), 981–990.
- Kalnay, E., Kanamitsu, M., Kistler, R., Collins, W., Deaven, D., Gandin, L., Iredell, M., Saha, S., White, G., Woollen, J., 1996. The NCEP/NCAR 40-year reanalysis project. *Bull. Am. Meteorol. Soc.* 77, 437–471.
- Knapp, K.R., Kruk, M.C., Levinson, D.H., Diamond, H.J., Neumann, C.J., 2010. The international best track archive for climate stewardship (IBTrACS) unifying tropical cyclone data. *Bull. Am. Meteorol. Soc.* 91, 363–376.
- Krishnamurti, T.N., 1979. *Tropical Meteorology*. Springer, New York.
- Kuo, Y.C., Lee, M.A., 2013. Decadal variation of winter-time sea surface temperature in the Taiwan Strait. *J. Mar. Sci. Technol.* 21, 117–123.
- Li, Q., Duan, Y., Yu, H., Fu, G., 2008. A high-resolution simulation of Typhoon Rananim (2004) with MM5. Part I: model verification, inner-core shear, and asymmetric convection. *Mon. Weather Rev.* 136, 2488–2506.
- Liu, C.-X., Wan, Q.-L., Liao, F., Zhao, Z.-K., 2012. Surface observations in the tropical cyclone environment over the South China Sea. *J. Trop. Meteorol.* 18, 263–274.
- Mcculloch, M., Culverwell, I., 2005. Comparison of Air-sea Latent Heat Fluxes from HadGAM1 and the NOC Climatology. Available: [http://icoads.noaa.gov/marcdat2/P\\_MikeMcCulloch.pdf](http://icoads.noaa.gov/marcdat2/P_MikeMcCulloch.pdf).
- Nan, S., Li, J., Yuan, X., Zhao, P., 2009. Boreal spring Southern Hemisphere annular mode, Indian Ocean sea surface temperature, and East Asian summer monsoon. *J. Geophys. Res. Atmos.* (1984–2012) 114, D02103/1.
- Park, S., Deser, C., Alexander, M.A., 2005. Estimation of the surface heat flux response to sea surface temperature anomalies over the global oceans. *J. Clim.* 18, 4582–4599.
- Shaluf, I.M., 2006. Disaster types in Malaysia: an overview. *Disaster Prev. Manag.* 15, 286–298.
- Shaw, R., Nguyen, H., Habiba, U., Takeuchi, Y., 2011. Overview and characteristics of Asian monsoon drought. *Commun. Environ. Disaster Risk Manag.* 8, 1–24.
- Uram, H., 2005. Meteorological modification method and apparatus CIP. Florida patent application 11/028, 968.
- Vongvisessomjai, S., 2009. Tropical cyclone disasters in the Gulf of Thailand. *Sonklanakarini J. Sci. Technol.* 31, 213–227.
- Wang, F., Meng, Q.J., Tang, X.H., Hu, D.X., 2013. The long-term variability of sea surface temperature in the seas east of China in the past 40 a. *Acta Oceanol. Sin.* 32, 48–53.
- Wang, L., 2008. Study of Tropical Cyclogenesis over the South China Sea. Unpublished PhD thesis. Hong Kong University of Science and Technology, Hong Kong.
- Wilks, D.S., 2011. *Statistical Methods in the Atmospheric Sciences*. Waltham, Academic press, Massachusetts.
- Xie, S.P., Deser, C., Vecchi, G.A., Ma, J., Teng, H., Wittenberg, A.T., 2010. Global warming pattern formation: sea surface temperature and rainfall. *J. Clim.* 23, 966–986.
- Yu, L., Weller, R.A., 2007. Objectively analyzed air-sea heat fluxes for the global ice-free oceans (1981–2005). *Bull. Am. Meteorol. Soc.* 88, 527–539.

- Yuan, J., Miller, R.L., 2002. Seasonal variation in precipitation patterns to the global ocean: an analysis of the GPCP version 2 data set. *Glob. Biogeochem. Cycles* 16, 50/1–50/10.
- Zeng, L., Shi, P., Liu, W.T., Wang, D., 2009. Evaluation of a satellite-derived latent heat flux product in the South China Sea: a comparison with moored buoy data and various products. *Atmos. Res.* 94, 91–105.
- Zhai, P., Zhang, X., Wan, H., Pan, X., 2005. Trends in total precipitation and frequency of daily precipitation extremes over China. *J. Clim.* 18, 1096–1108.
- Zhang, Y., Meng, Z., Zhang, F., Weng, Y., 2014. Predictability of tropical cyclone intensity evaluated through 5-year forecasts with a convection-permitting regional-scale model in the atlantic basin. *Weather Forecast.* 29, 1003–1023.
- Zong, H., Liu, Y., Xiu, P., Xu, Q., Rong, Z., 2010. Interannual variability of latent and sensible heat fluxes in the South China Sea. *Chin. J. Oceanol. Limnol.* 28, 153–159.
- Zuki, Z.M., Lupo, A.R., 2008. Interannual variability of tropical cyclone activity in the southern South China Sea. *J. Geophys. Res.* 113, D06106.1–D06106.14.